Molecular Dynamics Investigation of the ω-Current in the Kv1.2 Voltage Sensor Domains

Fatemeh Khalili-Araghi,[†] Emad Tajkhorshid,[‡] Benoît Roux,[§] and Klaus Schulten[†]

[†]Department of Physics, [‡]Department of Biochemistry, University of Illinois at Urbana-Champaign, Urbana, Illinois; and [§]Department of Biochemistry and Molecular Biology, University of Chicago, Chicago, Illinois

Supplementary Material

Comparison of pore-facing residues identified in simulations and in experiments

In a recent study Tombola et al (1) have identified residues of the VSD, the mutation of which affects the magnitude of the ω-current in the Shaker potassium channel. Experiments were performed by replacing each residue of the VSD with cystine, or by attaching positively or negatively charged MTSET or MTSES agents to cystine mutants. The magnitude of the current after residue modification was recorded, and the residues that affect the current significantly were reported by the authors.

Our simulations characterized the permeation pathway of the ions through the ω-pore differently than done in the experiment. Residues of the VSD that line the permeation pathway and interact with K^+ or Cl^- ions are identified and the strength of their interaction is quantified by the average time that permeating ions spend within 3 Å of the residue side chains. The residues identified in the simulation face the permeation pathway directly within the ω-pore, and their mutation (in particular to residues with bulky side chains with or without charged agents) is expected to affect the magnitude of the current. However, the reverse is not necessarily true. The experiments identify certain amino acid positions on the sequence of the VSD, where adding the bulky side chains affects the magnitude of the current through altering channel properties, but the native side chains do not need to face the conduction pathway for playing such a role.

Clear examples of this case are A359 and A355 in Shaker. These residues are identified in the experiments to affect the magnitude of the ω-current when mutated to cystine, with or without charged reagents. However, the simulations do not show direct interaction of these residues with the passing ions. The simulations have identified L358 and Q354 as the residues that interact with the passing ion that face the ω-pore (L290 and Q286 in Kv1.2). Side chain modification of L358 and Q354 are also known to affect the current in the experiments. So, while alanine side chains (359 and 355) are not facing the permeation pathway, it is quite obvious that attachment of a bulky molecule to their side chains will affect the magnitude of the currents measured in the experiments, as their neighboring residues interact closely with the permeating ion.

A similar argument can be made in the case of S357 (in Shaker), which is located right above L358 that is part of the constriction region in the pore.

The same is true for residues T284 and T329 (T184 and T272 in Kv1.2), which are located next to the high impact residues E183 (on S1) and E273 (on S3). Threonine residues (284 and 329) face away from the conduction pathway and have been identified to affect the current "indirectly" in the experiments. So, they would not appear as "interacting" residues in the simulation trajectories.

Cation Selectivity

The ω-pore in the Shaker K^+ channel is selective for cations (1), although selectivity has not been characterized quantitatively. The monovalent ions, Li^+, Na^+, K^+, and Cs^+ pass through the pore with a weak preference for the larger cations (2). Positively charged guanidinium ions also cross the membrane through the ω-pore, with a conductivity $\sim$8 times higher than that of other cations (2). The lack of strong ionic selectivity among cations (in contrast to the highly selective central conduction pore) suggests that there are no specific interactions between permeant ions and the protein side chains. Electrostatic interactions between the ions and protein residues govern the permeation pathway of the ions within the pore. The negatively charged residues located near the constriction region (E1D and E0) provide an energetic barrier for Cl^- ions. Electrostatic forces within the narrow constriction region, separating intra- and extracellular solutions, precludes permeation of Cl^- ions while attracting the positively charged K^+ ions lingering around the extracellular mouth of the VSD. The flexible nature of the VSD (reported in (3–5)) allows for expansion and contraction of the pore to accommodate larger or smaller cations, while excluding (to some extent) anions.

Molecular Dynamics Simulations

MD simulations were carried out using the program NAMD (6) and the CHARMM27 force field parameter set for proteins (7; 8), ions (9), and phospholipids (10; 11), with the TIP3P water model (12). All simulations were performed at constant temperature and constant pressure, with a fixed cross-sectional area for the membrane after the initial adjustment (NP_nAT ensemble) (13). Assuming periodic boundary conditions, the particle mesh Ewald (PME) method (14) with a grid spacing of $\sim$1 Å in each dimension was employed for the computation of long-range electrostatic forces. All simulations employed time steps of 1 fs, 2 fs, and 4 fs for bonded, non-bonded, and electrostatic calculations, respectively. Langevin dynamics with a friction coefficient of $\gamma = 5 \ ps^{-1}$ was used to keep the temperature constant. The Langevin piston Nosé-Hoover method (15) was employed to maintain the pressure at 1 atm, with a decay period of 100 fs and a time constant of 200 fs.

Simulated VSD	-0.25 V	-0.75 V	-1 V
R1N	1.5 Å	2.6 Å	3.5 Å
R1S	1.8 Å	3.1 Å	2.8 Å
E1D-R1N	2.1 Å	3.6 Å	3.1 Å
E1D-R1S	1.6 Å	3.4 Å	3.2 Å

Table S1: Average backbone RMSD of the four VSD mutants during equilibration at -0.25 V and the production runs at -0.75 V and -1 V relative to the initial protein conformation for each simulation. The RMSDs are calculated for the transmembrane region of the VSD, excluding the S1-S2 extracellular loop.
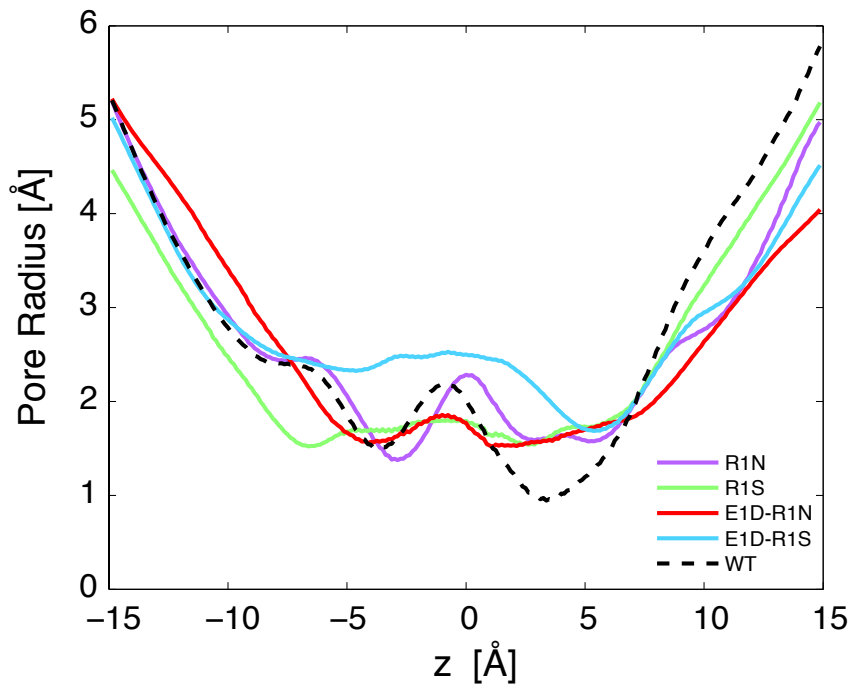
Figure S1: Pore radius profiles of the ω-pore in the Kv1.2 channel. The radius profile of the pore within the VSD is calculated using the program HOLE (16; 17) for the wildtype (WT) VSD and four of its mutants for the last 3 ns of the equilibration simulations. The pore radius profile is calculated along the membrane normal (z-axis) at every 10 ps of the trajectory and the averaged results are presented here.
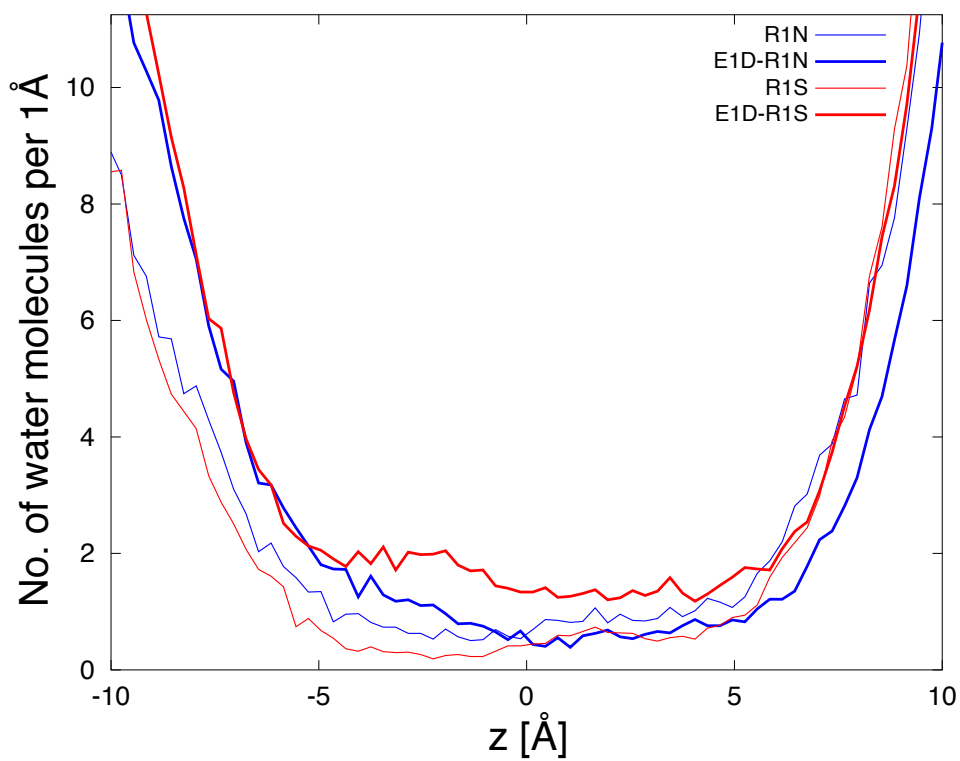
Figure S2: Water density profiles in the ω-pore of the Kv1.2 channel. The plot is normalized over the entire trajectory of the four mutants at $-1\,V$.

References

[1] Tombola, F., M. M. Pathak, P. Gorostiza, and E. Y. Isacoff. 2007. The twisted ion-permeating pathway of a resting voltage-sensing domain. *Nature.* 445:546–549.

[2] Tombola, F., M. M. Pathak, and E. Y. Isacoff. 2005. Voltage-sensing arginines in a potassium channel permeate and occlude cation-selective pores. *Neuron.* 45:379–388.

[3] Nishizawa, M. and K. Nishizawa. 2008. Molecular dynamics simulation of Kv channel voltage sensor helix in a lipid membrane with applied voltage. *Biophys. J.* 95:1729–1744.

[4] Bjelkmar, P., P. Niemelä, I. Vattulainen, and E. Lindahl. 2009. Conformational changes and slow dynamics through microsecond polarized atomistic molecular simulation of an integral kv1.2 ion channel. *PLoS Comput. Biol.* 5:e1000289.

[5] Khalili-Araghi, F., V. Jogini, V. Yarov-Yarovoy, E. Tajkhorshid, B. Roux, and K. Schulten. 2010. Calculation of the gating charge for the Kv1.2 voltage-activated potassium channel. *Biophys. J.* 98:2189–2198.

[6] Phillips, J. C., R. Braun, W. Wang, J. Gumbart, E. Tajkhorshid, E. Villa, C. Chipot, R. D. Skeel, L. Kale, and K. Schulten. 2005. Scalable molecular dynamics with NAMD. *J. Comp. Chem.* 26:1781–1802.

[7] MacKerell, A. D., Jr., D. Bashford, M. Bellott, R. L. Dunbrack, Jr., J. D. Evanseck, M. J. Field, S. Fischer, J. Gao, H. Guo, S. Ha, D. Joseph, L. Kuchnir, K. Kuczera, F. T. K. Lau, C. Mattos, S. Michnick, T. Ngo, D. T. Nguyen, B. Prodhom, I. W. E. Reiher, B. Roux, M. Schlenkrich, J. Smith, R. Stote, J. Straub, M. Watanabe, J. Wiorkiewicz-Kuczera, D. Yin, and M. Karplus. 1998. All-atom empirical potential for molecular modeling and dynamics studies of proteins. *J. Phys. Chem. B.* 102:3586–3616.

[8] MacKerell Jr., A. D., M. Feig, and C. L. Brooks III. 2004. Extending the treatment of backbone energetics in protein force fields: Limitations of gas-phase quantum mechanics in reproducing protein conformational distributions in molecular dynamics simulations. *J. Comp. Chem.* 25:1400–1415.

[9] Beglov, D. and B. Roux. 1994. Finite representation of an infinite bulk system: Solvent Boundary Potential for Computer Simulations. *J. Chem. Phys.* 100:9050–9063.

[10] Schlenkrich, M., J. Brickmann, A. D. MacKerell Jr., and M. Karplus. 1996. Empirical potential energy function for phospholipids: Criteria for parameter optimization and applications. In K. M. Merz and B. Roux, editors, *Biological Membranes: A Molecular Perspective from Computation and Experiment.* Birkhauser, Boston, pages 31–81.

[11] Feller, S. E. 2000. Molecular dynamics simulations of lipid bilayers. *Curr. Opin. Coll. & Interf. Sci.* 5:217–223.

[12] Jorgensen, W. L., J. Chandrasekhar, J. D. Madura, R. W. Impey, and M. L. Klein. 1983. Comparison of simple potential functions for simulating liquid water. *J. Chem. Phys.* 79:926–935.

[13] Feller, S. E. and R. W. Pastor. 1999. Constant surface tension simulations of lipid bilayers: The sensitivity of surface areas and compressibilities. *J. Chem. Phys.* 111:1281–1287.

[14] Darden, T., D. York, and L. Pedersen. 1993. Particle mesh Ewald. An N·log(N) method for Ewald sums in large systems. *J. Chem. Phys.* 98:10089–10092.

[15] Martyna, G. J., D. J. Tobias, and M. L. Klein. 1994. Constant pressure molecular dynamics algorithms. *J. Chem. Phys.* 101:4177–4189.

[16] Smart, O., J. Goodfellow, and B. Wallace. 1993. The pore dimensions of Gramicidin A. *Biophys. J.* 65:2455–2460.

[17] Smart, O. S., J. G. Neduvelil, X. Wang, B. A. Wallace, and M. S. P. Sansom. 1996. HOLE: A program for the analysis of the pore dimensions of ion channel structural models. *J. Mol. Graphics.* 14:354–360.